

# IMPROVEMENT OF PRINTING QUALITY THROUGH SATELLITES FORMATION CONTROL

Ilaria Valenti\*, Myriam Vicari, Paolo Casarini

Research and Development laboratory, System Ceramics, Decoration department, System S.p.A., Via Ghiarola Vecchia 73 Fiorano Modenese (Modena) – Italy.

### 1. ABSTRACT

This work describes a method to improve printing quality through the control of satellite formation mechanism, which is a direct consequence of drop formation process. The method is based on a model presented and experimentally verified in a previous study [1], relating drop velocity to satellite number through tail length at the detachment from nozzle. A brief presentation of the model for single event condition is introduced, then the model is here generalised including frequency effects. A parameter to evaluate printing quality a priori, from ink and printhead properties, is introduced and the dependence from single relevant quantities is highlighted. Actual example of tuning of ink properties is presented and the effect on drop formation are experimentally analysed. A very general method to improve printing quality is proposed, which is applicable to each printing system, opening the way to the possibility to create modellable fluids with the best printing performances.



# 2. INTRODUCTION

Drop-on-demand piezoelectric inkjet printing represents nowadays one of the most diffused decoration technologies thanks to its high performance and reliability [1 - 5]. To reach the goal of high quality, many different requirements have to be met in terms of drop properties, leading to a very precise dot positioning and thus to a high quality final image. In industrial ceramics application many complexities are introduced, i.e. the need for a moving support and the request for higher and higher line speeds. The satisfaction of industrial efficiency without affecting printing quality and process reliability is a hard task that requires an excellent knowledge of involved devices and technologies, but also concerning inks properties. In particular, a deep understanding of the role and interaction of inks and printheads in drop formation is fundamental to gain a high control of the whole process.

The most crucial property is drop velocity: a high precision in dot positioning requires a high drop speed, especially when working at a high distance from the support is needed; a fast drop is also less affected by positioning errors due to a high line speed. To obtain an excellent printing quality, it is also fundamental to reduce satellites number or they have to be fast enough to reach main drop before landing on the support. Satellites speed depends strongly on rheological ink properties; drop speed depends on ink properties [6] and on nozzle geometry [7], but can also be varied by acting on firing conditions such as firing pulse [8]. The faster the drop is, the harder the junction with satellites during flight is [9]. The goal of a high printing quality is the result of a compromise between the need of a fast drop for a good dot positioning, and the reduction of satellite number to minimum. A deep analysis of drop formation is thus required to gain an excellent knowledge of the relationship between the different factors leading to final result.

Many studies have analysed drop dynamics considering the different stages of drop formation from both an experimental and theoretical point of view [10-18], however an accurate description of the relationship between drop speed and satellites dynamics is still missing. This relationship is fundamental not only to comprehend the system, but also to evaluate the best working conditions in industrial application and thus to reach the goal of a high printing quality.

In our previous study [1], we described the relationship between the fundamental properties for application with a very general model, applicable to each system. The model has been verified through experimental analysis of different printheads-ink combinations in a simplified condition allowing to exclude frequency effects.

In this work, after an introduction on drop formation and on the previously developed model, we extend the results to the more complex yet fundamental case, where the effects of frequency are not negligible, which corresponds to the actual situation in laboratory and especially in industrial production.

The generality of the model and its perfect match with the experimental data allows to introduce a parameter to evaluate printing quality *a priori*, simply considering ink rheological properties and printhead nozzle size. A very general and easily applicable procedure is proposed to modify ink properties to improve printing performances. The procedure is tested on different systems and some relevant considerations are drawn.



# 3. EXPERIMENTAL SETUP

In our works ten combinations of printheads and inks have been analysed. The first seven combinations have been considered in the first work [1] to validate the model. Other combinations have been added in this study to analyse frequency effect and to test the method of performance improvement. Combinations are labelled with a number and a letter.

Piezoelectric printheads working in shear mode have been used; we considered three different nozzle diameters (d):A) 33 µm, B) 41 µm and C) 56 µm. Drops are jetted top-down, with printhead in vertical position. In the involved process, gravitational forces are negligible. Various inks have been analysed, whose properties, namely density ( $\rho$ ), viscosity ( $\eta$ ) and surface tension ( $\gamma$ ), have been measured at System Laboratory. Relevant properties for each combination are reported in Table 1.

	d	ρ	η	Y	Oh	Re
	(µm)	(kg/m³)	(mPa s)	(mN/m)		5 m/s
1A	33	1062	11.3	22.6	0.40	8
2A	33	1084	12.3	20.8	0.45	7
3B	41	1310	14.6	27.3	0.38	9
4B	41	1175	14.7	26.4	0.41	8
5C	56	1500	16.4	26.0	0.35	13
6C	56	1253	17.5	28.8	0.39	10
7C	56	1182	17.5	28.1	0.41	10
8B	41	1043	11.5	21.9	0.27	9
9B	41	950	10.2	31.0	0.32	10
10A	33	1114	15.7	34.3	0.44	6

**Table 1**.Properties of the analysed combinations: nozzle diameter (d), ink density ( $\rho$ ), viscosity ( $\eta$ ) and surface tension ( $\gamma$ ).Ohnesorge (Oh) and Reynolds (Re) number at 5 m/s are also reported.

Proper printheads working conditions require viscosity between 6 and 20 mPas and surface tension between 20 and 45 mN/m. Ink properties have been measured at working temperature, which vary between 35°C and 50°C. Table 1 shows calculated Ohnesorge (Oh) and Reynolds (Re) numbers for each combination. Reynolds number has been determined for a typical fluid speed of 5 m/s. Both Oh and Re satisfy the requested conditions for proper jetting:  $0.1 \le Oh \le 1$  [3, 19] and Re > 2/Oh [3]. Due to



the printhead requirements, ink properties range is quite narrow and leads to common behaviours, nonetheless variations of properties are allowed and a fine control of the system is possible.

Experimental analysis has been conducted with a printhead testing bench, reproducing an industrial digital printing machine in terms of both hydraulic and electric circuit. Drop speed and tail length have been measured by a Drop Watcher JetXpert System, detecting drop motion with a fire wire camera and a stroboscopic LED light.

A single trapezoidal positive pulse (Fig.1a) actuated piezoelectric heads. Pulse properties, namely duration ( $\Delta t = t_{rise} + t_{dwell}$ ) and voltage (V) have been changed to vary drop formation conditions. Duration was chosen to maximise drop speed at a fixed reference voltage. Specific duration values for each combination depend on ink and printhead properties ( $4 \ \mu s \le \Delta t \le 12 \ \mu s$ ), but they all correspond to the same working condition of optimal pressure wave synchrony. With duration kept fixed, voltage applied to printheads has been changed to obtain different drop speed ( $65 \ V \le V \le 120 \ V$ ). Pulse slope was 40 V/ $\mu s$ . Firing frequency has also been varied. "Single event condition" has been considered, corresponding to 0.5 kHz frequency, which is sufficiently low to exclude interaction between subsequent pulses. To analyse drop behaviour in frequency domain, we varied jetting frequency between 0.5 and 20 kHz.

Obtained images have been analysed by ImageXpert software (Fig.1b-c), which allows to measure lengths. Drop speed and tail length have both been measured at the detachment of tail from nozzle. Drop velocity was determined via software considering two images of the same drop with 5 ns between the acquisitions and calculating space over time ratio. Errors on drop speed and tail length have been evaluated to be  $\pm 0.5$  m/s for drop speed and  $\pm 0.05$  mm for tail length, respectively, considering drop oscillations and operator contribution.

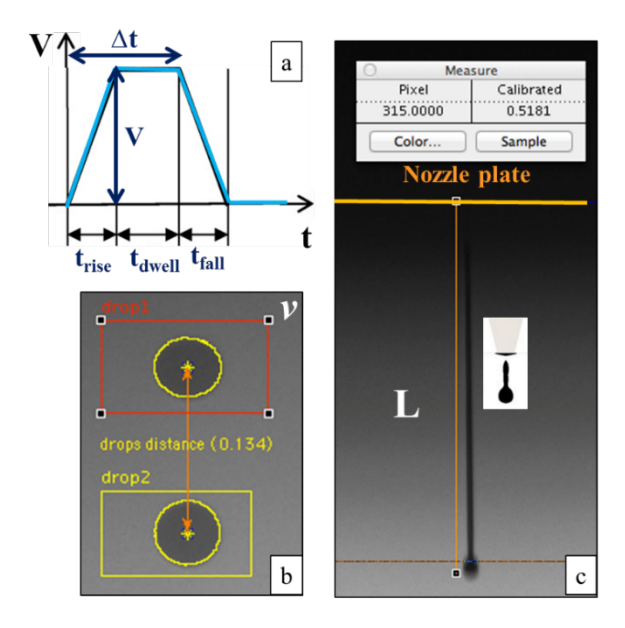


**Fig.1. a)** schematic representation of single trapezoidal pulse used in the analysis. b) drop speed and c) tail length measurement performed by Drop Watcher.



# 4. DROP FORMATION

We present a brief description of drop formation we developed by combining literature research [1-18] and our direct analysis of the specific system in study.

Six main phases can be identified considering a drop emerging from a nozzle [12]:1) ink is ejected from nozzle, 2) it stretches outside nozzle and tail is formed and 3) two necking point are identified, between tail and nozzle and between drop and tail.4) Then, tail detaches from nozzle (pinch-off) and 5) drop recoils. Finally 6) tail breakups, leading to satellites formation.

Fig.2 shows the main phases of drop formation detected by Drop Watcher for the system in analysis in this study (combination 1A).In Fig.1a zero point is shown (nothing happens), then ink is ejected from nozzle (b) and elongates forming a tail, which detaches from nozzle (c).Tail and drop move away from nozzle plate and at a certain point breakup occurs (d-f), with the formation of satellite droplets which are slower and smaller than main drop.

After tenths of microseconds pulse ends, liquid flux to nozzle decreases and the difference in fluid speed between the opposite ends of liquid jet causes the formation of tail, which elongates and decelerates due to dissipation by viscous forces [12,16]. Soon after the stretching stage, the higher capillary pressure at necking point between tail and nozzle causes the detachment of tail from nozzle, known as pinch-off. The formation of the drop-tail system ends with pinch-off, which represents a crucial phase affecting all following drop motion. After pinch-off tail recoils due to asymmetry in the liquid column. While moving away from nozzle tail eventually divides into satellites: the most common process is Rayleigh breakup [10], but also different processes, are possible, such as fast or low satellite formation.

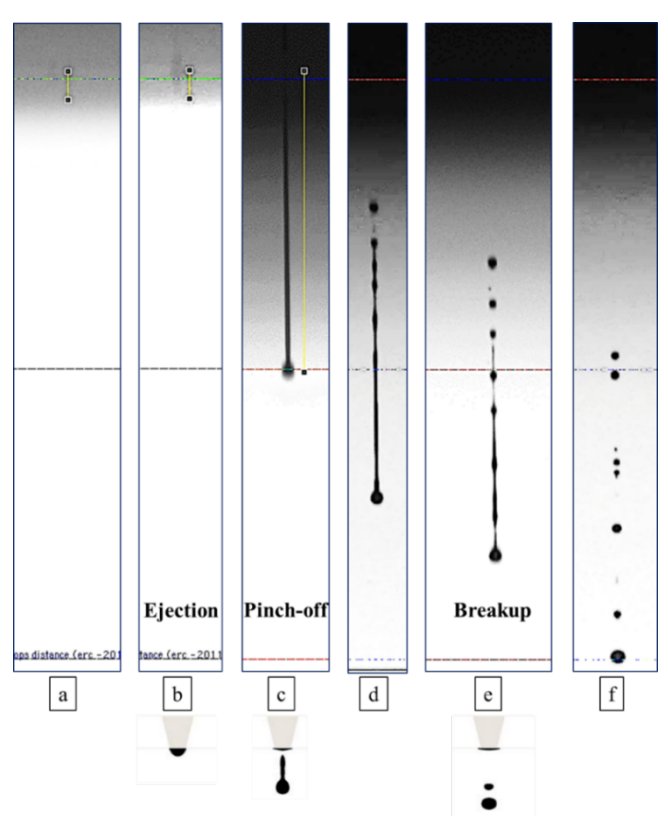


**Fig.2.** Phases of drop formation for combination 1A observed with DropWatcher ( $V=92\ V$ ,  $\Delta t=5\ \mu s$ , frequency=0.5 kHz).



Breakup mechanism depends on ink and printhead properties [2], in particular jet stability can be analysed in term of *Oh* number and jet aspect ratio (diameter over length)[20-21]. Considering the systems analysed in this study, *Oh* is about 0.3-0.4, and minimum aspect ratio is 25: coherently with these data, Rayleigh breakup was always observed for all combinations in all firing conditions. As previously mentioned, the common range of properties lead to some common aspects, such as breakup mechanism.

Drop speed at ejection is determined by pulse properties, namely voltage and pulse duration. While duration is responsible for pressure wave superposition [2, 11, 22], voltage acts on the energy transmitted to drop. In our study, we considered the same condition in terms of wave superposition choosing optimal duration, then we varied voltage to obtain different speed values.

All the previous considerations are valid in single event condition, namely when jetting frequency is so low that each event is independent from the previous one and does not affect the subsequent one. When frequency is higher than a critical value, some other effects have to be considered, related to superposition and interference of residual waves and the new jetting wave.

# 5. DROP SPEED AND SATELLITE NUMBER

In our previous study [1], we analysed drop formation for seven different ink-printheads combinations, namely combinations from 1A to 7C.As described in the previous section, satellite formation always occurs by Rayleigh breakup, due to printhead and ink properties. Most studies on satellites reduction focus on breakup process [13, 16, 23-24]; actually, pinch-off is the crucial moment on which all following phases depend. Satellite number is directly connected to tail length at pinch off, which, in turn, depends on drop speed: in this paragraph, we describe a simple model, which relates those fundamental quantities.

For the considered systems, we identified a phenomenological relation between tail length and satellite number. In particular, the longer the tail at detachment is, the higher the number of satellites at a certain distance from nozzle is. Table 2 shows numerical results for combination 1A, reporting tail length L and number of satellites counted when drop is 2 mm far from plate. Since Rayleigh breakup is a non-repeatable process, satellite number is the result of 15 repetitions of the measurement: minimum and maximum values have been reported. Similar results have been obtained for all combinations: satellite number increases with tail length: tail length at detachment from nozzle represents a crucial parameter to determine printing quality.



L (mm)	Satellite number		
0.24	0		
0.30	0 - 1		
0.39	1 - 3		
0.43	1 - 4		
0.50	7 – 9		
0.66	10		

**Table 2.** Tail length at pinch-off and corresponding number of satellites observed when drop reaches a distance of 2 mm from nozzle plate.

In our study [1], starting from the analysis of Li et al.[25], we elaborated the following relation:

L = a k v = m v Where:

$$k = \sqrt{\frac{d}{\rho \gamma^3}} \eta^2$$

A variation in voltage leads to different (v,L) couples, describing a straight line, whose slope m=ak depends on ink density, viscosity and surface tension, and on nozzle size. The smaller the slope is, the shorter the tail will result, at fixed speed. In this formulation, dependences on ink and printhead properties are included in constant k, which can be calculated for each system a priori. Parameter a is an unknown non-dimensional quantity, expected to be constant in the ideal circumstances. Slope m can also be seen as the time drop needs to cover distance L moving with uniform linear motion at fixed speed v, namely speed at pinch-off. Actually drop speed is not constant: drop is highly accelerated at ejection, then motion is decelerated due to tail drag. We call m the "ideal formation time", k "printhead-ink combination time" and a "velocity factor".

The obtained relation has been experimentally verified. Printhead-ink combination time k has been calculated for each combination starting from properties in Table 1; from error propagation, k uncertainty can be set to 15%. Combination time values are reported in Table 3. The measured (v,L) couples are shown in Fig.3a, with the corresponding linear fits. Measurements have been performed in single event condition (0.5 kHz). All trends are linear, with zero intercept and  $R^2$  ranging from 0.95 to 0.99. Slopes of the straight lines, whose numerical values are reported in Tab.3, follow the same trend of k values. The agreement of trend is not trivial, since combination time has been determined a priori from ink and printhead properties, while ideal formation time has been determined independently, from linear fit of experimental data. It can be noticed that dependence on nozzle size is very relevant.



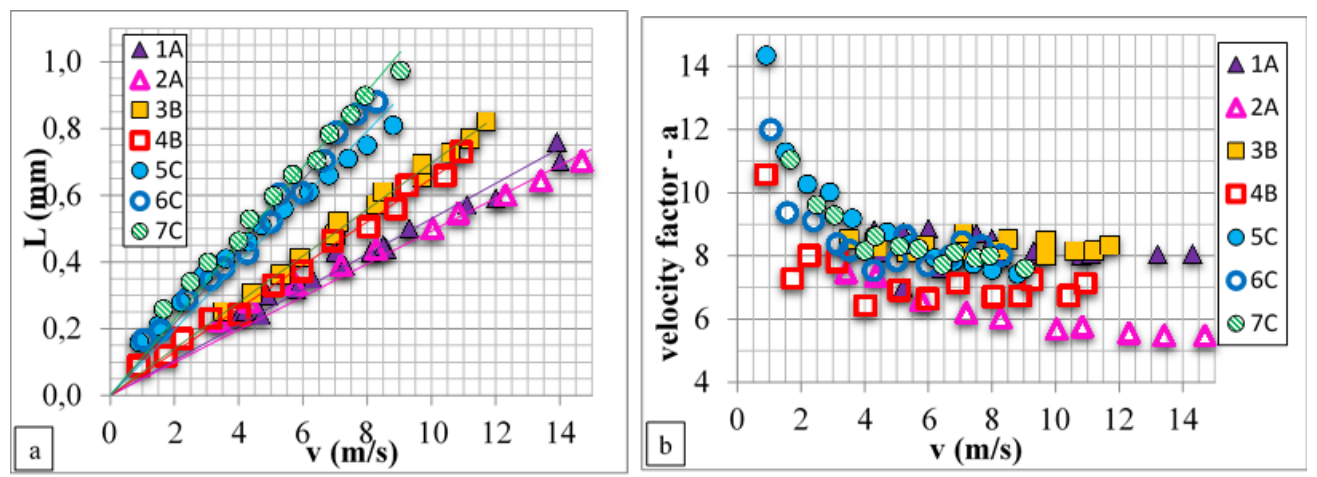


**Fig.3:** Experimental validation of the model at frequency 0.5 kHz. a) Tail length as a function of drop speed at pinch-off. b) Velocity factor a for each (v,L) couple as a function of drop speed.

#	k (µs)	m (µs)	a
1A	7	49	7
2A	9	53	6
3B	8	65	8
4B	9	70	8
5C	12	99	8
6C	13	110	8
7C	14	111	8

**Table 3:** k, m and a values obtained for the analysed combinations. Combination time k has been calculated from ink and printhead properties, slope m has been determined by linear fit and velocity factor a has been calculated as m/k ratio.

Velocity factor a can be calculated as the ratio between slopes determined by fit and k values calculated a priori: values ranges from 6 to 8, with estimated uncertainty of 20% (Tab.3). Velocity factor is thus independent from the ink-printhead properties.

Single a values can also be calculated for each (v,L) couple (Fig.3b) as m/k ratio with m values obtained as L/v ratio. Values reported in Fig.3b are almost constant for speed higher than 4 m/s, while for low speed ratio rapidly decreases with increasing drop velocity. Any clear distinction between different nozzle size is removed, with removal of dependence on ink-printhead combination obtained dividing by k.

In the proposed model, velocity factor was expected to be independent from combination and speed. The non-constant observed trend for velocity factor at low



speed could be explained considering drop velocity variation during motion. Drop motion is not uniform: it is highly accelerated soon after ejection and suffers a deceleration in following times. Velocity factor a describes the effect of speed variation during motion and is independent from ink-printhead properties, which are included in k constant. All analysed combinations, regardless of difference in fluid properties and nozzle geometry show the same value and superimposed trends.

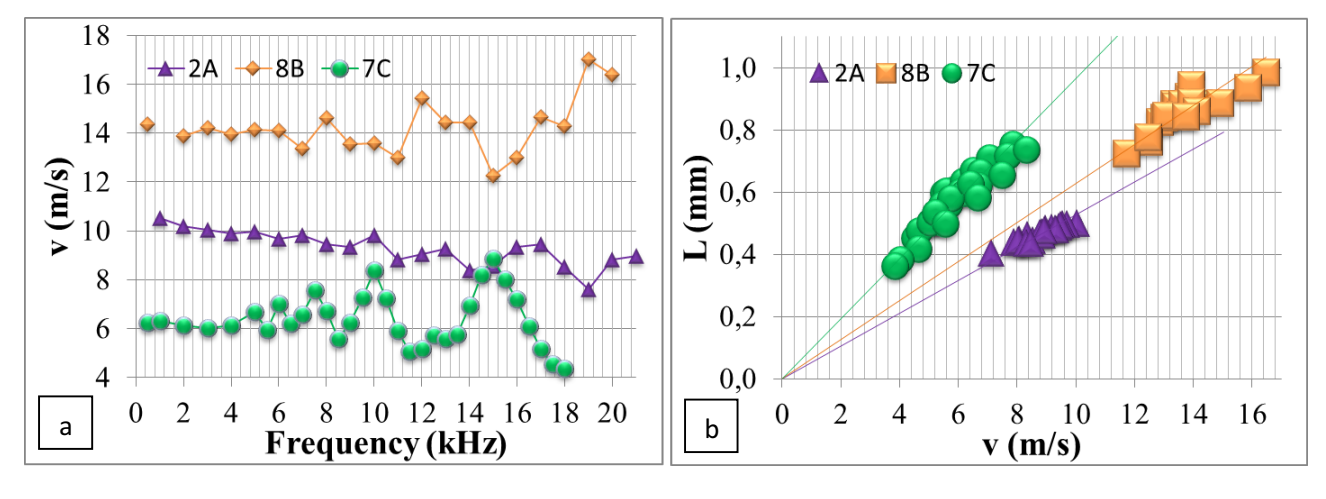
# 6. FREQUENCY DOMAIN

The analysis described so far is valid in single event conditions, when frequency is sufficiently low that meniscus has enough time to relax between one jetting event and the subsequent. On the contrary, if frequency overcomes a certain critical value, superposition of waves and interference affect drop formation. Viscous forces at nozzle damp residual oscillations: the bigger the nozzle is, the lower the damping effect is; thus, frequency effects are particularly relevant for big nozzle diameter.

To analyse the effect of frequency on tail length-drop speed relation, three combinations with different nozzle diameter have been considered and analysed varying jetting frequency between 0.5 and 20 kHz. Relevant properties and calculated k values are reported in Table 4.

	Oh	Re 5 m/s	k (µs)
2A	0.45	7	9
8B	0.27	9	8
7C	0.41	10	14

**Table 4:** Properties of combinations considered for analysis in frequency. Calculated Oh, Re and k values.



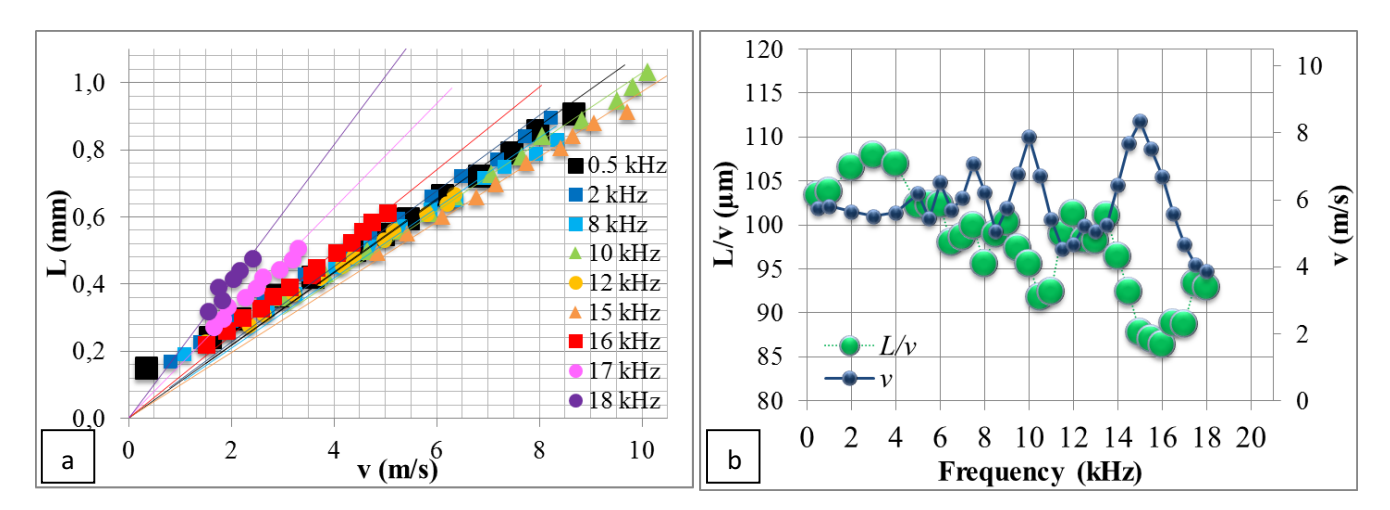
**Fig.4:**Analysis in the frequency domain. a) Drop speed at pinch-off as a function of frequency. b) Tail length L as a function of drop speed; all data for different frequencies are reported.



Fig.4a shows the velocity trend as a function of frequency: drop speed shows maxima and minima related to constructive and destructive interference between waves in the channel. Oscillation amplitude is lower for smaller nozzle size, as expected. In Fig.4b all available data on (v,L) couples at different frequencies are reported: the linear relation between tail length and drop speed is verified with experimental error taken into account. Nonetheless, some deviations from straight line are observed, more relevant for systems with bigger nozzle size.

To get a deeper comprehension of the frequency role, 7C combination has been considered, where frequency effects are stronger due to the bigger nozzle diameter.(v,L) couples have been measured at different frequencies, keeping frequency constant for each data serie and varying voltage to obtain different drop speed values (Fig.5a). For frequency lower than 10 kHz very small variations are observed, corresponding to a quite constant drop speed as a function of frequency (Fig.5b).

A comparison between drop speed with L/v ratio as a function of frequency shows that maxima in the first trend correspond to minima in the second (Fig5b). Similarly, slope of the straight line reflects the same behaviour: considering for example 15 kHz frequency, speed shows a maximum and slope of L/v trend reaches a minimum; with voltage kept fixed speed increases from 5.4 m/s to 8.4 m/s and ideal formation time reduces from 109 to 97  $\mu$ s. With increasing frequency speed oscillations are more pronounced, and variations in slopes are higher: at 18 kHz a tail length of 0.4 mm is obtained with speed of 1.8 m/s, while in single event same tail length is observed with double drop velocity.



**Fig.5: a)** Tail length L as a function of drop speed v at different frequencies value for combination 7C. Linear fit with zero intercept are also reported. b) L/v and drop speed trends as a function of frequency, for combination 7C at fixed voltage ( $V=105\ V$ ).

The effect of frequency, namely constructive or destructive interference, causes the well known variation in drop speed. The linear relation between drop speed and tail length is nonetheless maintained, with small changes in slope due to velocity oscillations rather than to a different drop formation mechanism. These effects are particularly relevant for big nozzle size and high frequency, while for small nozzle diameter and low frequencies, interference effects are almost negligible.



# 7. GENERALISATION OF THE MODEL

We showed that the simple linear equation relating tail length to drop speed at pinch off is valid not only in single event condition, but also when frequency effects are included in the picture. The mechanism of tail formation is not affected by frequency, only slope varies due to speed oscillation, by a factor depending on interference effects.

The drop speed-tail length model can thus be generalised including frequency contributions.

Considering the relation L = mv, in single event condition m = ak, with combination time k depending on ink and printhead properties and constant velocity factor a, including speed variation due to change in drop velocity from ejection to pinch-off.

In multiple event case, namely when frequency is so high that interference effect have to be considered, the equation can be rewritten as: L = abkv (m = abk).

The non-dimensional b factor is added, including frequency effect and depending on frequency itself. In single event condition b=1; |b-1| represents the relative variation with respect to single event case. We named b the "frequency factor".

Table 5 shows the resulting numerical values of involved quantities for combination 7C. Ideal formation time m has been determined by linear fit from graph in Fig. 5a, frequency factor have been calculated as b = m/(ak), where  $k = 14 \mu s$  and a = 8.

f (kHz)	m (µs)	b	b-1
0.5	109	1.00	0
2	113	1.04	0.04
8	104	0.95	0.05
10	103	0.94	0.06
12	108	0.99	0.01
15	97	0.89	0.11
16	124	1.14	0.14
17	157	1.44	0.44
18	204	1.87	0.87

**Table 5:** Values obtained for combination 7C at different jetting frequencies f.m values have been determined by linear fitting procedure of experimental data; b values have been calculated as the ratio between the determined m and the product ak =  $8 \times 14 \ \mu s = 112 \ \mu s$ . |b-1| represents the percentage variation with respect to single event condition.



# 8. IMPROVING PRINTING QUALITY

In our study, we showed a simple relation directly connecting satellite number and drop speed, which are the main factors on printing quality control. A compromise is needed to obtain a high drop speed and a reduced satellite number, which can be achieved by acting on the known relevant properties. The model is applicable in single event condition, but it has also been proven valid in frequency domain.

The introduced combination time k, whose value can be easily calculated for each printing systems and ink, allows an evaluation of printing quality a priori, known ink density, surface tension and viscosity, and nozzle size. In real application, i.e. in the ceramic market, considering a specific printing system, with a specific printhead and thus a fixed nozzle size, it is possible to modify ink properties to gain better performances. In ceramic application, it is often hard to act on density, but surface tension and viscosity can be changed to obtain the desired result. This leads the way to the development of modellable inks, whose properties are exactly tuned to respond to a specific request in terms of performances.

We tested the developed method considering two possible modifications in inks properties: viscosity and surface tension. Ink data and results are reported in Table 6-7 and Fig.6a-b.

Starting from combination 9B, we obtained a modified version of the ink, with lower viscosity. The slope of the  $\it L$  trend versus drop speed also reduces significantly, so that, for example, a speed of about 10 m/s corresponds to a tail length of 0.4 mm instead of 0.6 mm. On the other hand, a tail length of 0.4 mm is obtained with a drop speed of 10 m/s instead of 7 m/s.

Slope of the trend is also expected to suffer a reduction when increasing surface tension.

Ink in combination 9A has been modified with proper surfactants to obtain a version of the fluid with higher surface tension, and one with lower surface tension. In this case all three trends are quite superimposed and there is no significant difference between slopes, even if k value is significantly changed.

	η (mPa s)	Oh	Re 5 m/s	k (µs)	m (µs)
9B	10.2	0.32	10	50	60
9B - low viscosity	7.1	0.22	14	25	39

**Table 6:** Properties of combinations 9B with different viscosity: viscosity, and calculated Oh, Re, k and m values.



	Y (mN/m)	Oh	Re 5 m/s	k (µs)	m (µs)
10A	34.3	0.44	6	7	49
10A - low surface tension	26.1	0.51	6	10	49
10A - high surface tension	42.8	0.40	6	5	48

**Table 7:** Properties of combinations 10A, with modified surface tension: surface tension, and calculated Oh, Re, k and m values.

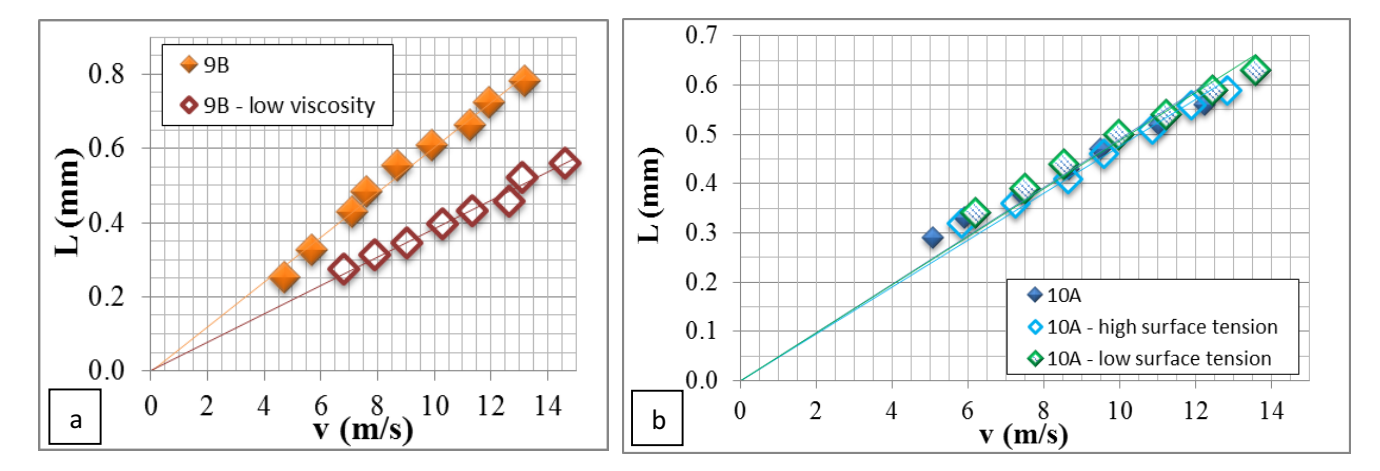


**Fig.6:** Tail length L as a function of drop speed v at different frequencies value and linear fits: a) combination 9B and b) combination 10A with considered inks modifications.

To understand the apparent discrepancy between expected slope reduction and the actual trend when surface tension is varied, measured surface tension has to be deeply considered. Fig.7 shows surface tension trend detected with a bubble pressure tensiometer for bubble lifetime ranging from 0.015 and 15 seconds. When mentioning surface tension for an ink, it is common to consider the so called "static" value, which means the value obtained for long bubble lifetime (in this case 15 s). However, the processes involved in this study, namely drop ejection and formation, involve much smaller timescales: drop formation is completed (pinch-off) in about 50  $\mu$ s, so this bubble lifetime has be considered.

In the 20-80  $\mu$ s bubble lifetime range, the difference between surface tension values is quite low, so it is not surprising that drops behaviour is almost the same. A surfactant acting on the short bubble lifetime range is in this case more suitable to obtain the desired results.



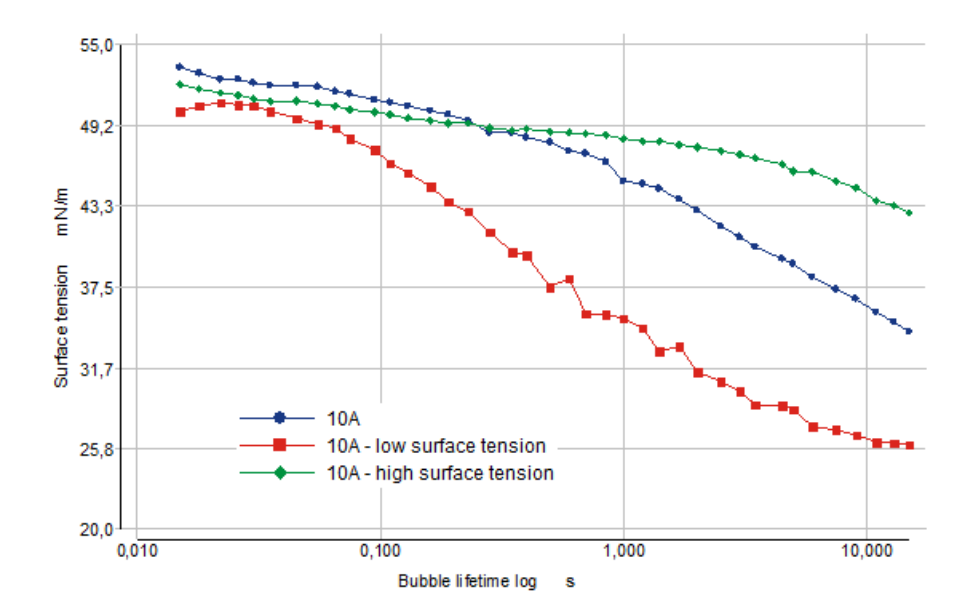


**Fig.7:** Surface tension data for the three formulation of ink 10 measured with a bubble pressure tensiometer for bubble lifetime between 15 μs and 15 s.

Surface tension is a dynamic quantity, thus the proper timescale has to be considered accordingly to the considered phenomena. Surface tension at high bubble lifetime value is suitable for slow processes such as meniscus management or nozzle plate wetting, while for drop jetting, which is much faster, shorter bubble lifetimes are more appropriate. When modelling an ink it is fundamental to consider the proper range of application, to act in the proper way on relevant properties.

## 9. CONCLUSIONS

In our study, we developed a simple model, which relates the two main actors in determining printing quality: drop speed and satellite number. Satellite number directly depends on tail length at detachment, whose relation with drop velocity is a simple linear equation depending on ink properties and printhead geometry.

We elaborated the model, describing all the relevant quantities involved and their physical meaning, then we verified the relation by the experimental analysis of various ink-printhead combinations. The combination time is a representative parameter for the system, which can be calculated *a priori* for each ink and printhead combination. The generality of model was confirmed on both single event condition and through frequency domain. Frequency acts on specific speed values, but the relation with tail length is linear at frequency between 0.5 and 20 kHz.

Finally, we proposed a straight and general method to improve printing quality acting on ink properties during formulation to gain the better performances in terms of drop speed and satellite number. We tested the method confirming its validity and deeply analysing how a modellable ink can be obtained. The power of this model lies in its generality and in the possibility to apply it to every system in a very simple and direct way.



#### **10. ACKNOWLEDGEMENTS**

This work was financially supported by System S.p.A. (Fiorano Modenese, Italy). The authors would like to acknowledge all the people collaborating to the proper functioning of the experimental setup, in particular all the technicians and software, materials and chemical engineers working at R&D Ceramic Decoration laboratories.

#### 11. **BIBLIOGRAPHY**

- [1] I. Valenti, M. Pifferi, R. Cagnoli and P. Casarini, Experimental study on the dependence of tail length on drop speed in piezo-inkjet printing (under review).
- [2] H. Wijshoff, Phys. Rep., vol. 491, no. 4, pp. 77-177, 2010.
- [3] I. Hutchings and G. Martin, Inkjet Technology for Digital Fabrication, Wiley, 2013.
- [4] J. Pond, Inkjet Technology and Product Development Strategies, Torrey Pines Research, 2000.
- [5] L. Hue, J. Imaging Sci. Techn., vol. 42, no. 1, pp. 49-62, 1998.
- [6] B. Gans, et al., Macromol. Rapid. Commun., vol. 26, no. 4, pp. 310-314, 2005.
- [7] D. Bogy and P. Talke, IBM J. Res. Dev., vol. 28, no. 3, pp. 314-321, 1984.
- [8] H. Wu and H. Lin, Mater. Trans., vol. 51, no. 12, pp. 2269-2276, 2010.
- [9] H. Wijshoff, Proc.Nanotech., vol. 3, p. 448, 2007.
- [10] L. Rayleigh, Proc. London Math. Soc., vol. 10, no. 1, pp. 4-13, 1879.
- [11] D. Bogy, Annu. Rev. Fluid. Mech., vol. 11, pp. 207-228, 1979.
- [12] H. Dong, W. Carr and J. Morris, Phys. Fluids, vol. 18, no. 7, pp. 01-16, 2006.
- [13] J. Eggers, Rev. Mod. Phys, vol. 69, no. 3, pp. 865-930, 1997.
- [14] A. Yang et al., J. Micromech. Microeng., vol. 16, no. 1, pp. 180-188, 2006.
- [15] J. Lai, J. Lin and K. Linliu, J. Micro/Nanolith. MEMS MOEMS, vol. 9, no. 3, 2010.
- [16] W. van Hoeve et al., Phys. Fluids, vol. 22, no. 12, 2010.
- [17] G. Martin, S. Hoath and I. Hutching, J. Phys.: Conf. Ser., vol. 105, 2008.
- [18] [18] J. Eggers and E. Villermaux, Rep. Prog. Phys., vol. 71, no. 3, 2008.
- [19] [19] M. Dondi et al., Proceedings of the 14th World Congress on Ceramic Tile Quality, QUALICER 2014, Castellón (Spain).
- [20] A. A. Castrejon-Pita et al., Phys. Rev. Lett., vol. 7, no. 074506, p. 108, 2012.
- [21] T. Driessen et al., Phys. Fluids, vol. 25, no. 062109, 2013.
- [22] J. Dijksman, Flow Turb. Combust., vol. 61, pp. 211-237, 1999.
- [23] T. Kowalewski, Fluid Dyn. Res., vol. 17, no. 3, pp. 121-145, 1996.
- [24] A. Lakdawala et al., Chem. Eng. Sci., vol. 130, pp. 239-253, 2015.
- [25] R. Li et al., Exp.Therm. Fluid Sci., vol. 32, no. 8, pp. 1679-1686, 2008.